JOURNAL OF GUIDANCE, CONTROL, AND DYNAMICS
Vol. 15, No. 6, November-December 1992

Design and Robustness Issues for Highly Augmented Helicopter Controls

Stephen Osder* and Donald Caldwell†
McDonnell Douglas Helicopter Company, Mesa, Arizona 85205

The paper discusses design procedures for achieving a multiple-input, multiple-output, fly-by-wire flight control system for helicopters. It defines an interpretation of "highly augmented" as requiring tight stabilization of all commanded states, including automatic trimming. Design procedures are given that provide physical insights into how control decoupling and desired bandwidths are achieved, using a contemporary attack helicopter as the model. A high-gain, explicit model-following system is shown to meet practical robustness criteria that are designed to validate performance and stability when extremes of the helicopter nonlinear dynamics become part of the control problem. Comparison of this system's performance with published "optimal" designs based on the same high-order, linear helicopter model is made, showing that these other designs will not meet the proposed practical robustness tests.

Nomenclature

A = plant matrix
B = control distribution matrix
B_P = partitioned B matrix
C = measurement matrix
F = feedforward transfer function
$G_c(s)$ = controller transfer function
$G_m(s)$ = model transfer function
h = altitude, ft
$H(s)$ = plant transfer function
K_C = attitude gain matrix
K_I = integral gain matrix
K_P = proportional gain matrix
p = body-axis roll rate, rad/s
q = body-axis pitch rate, rad/s
r = body-axis yaw rate, rad/s
S_I = inner-loop feedback matrix
S_O = outer-loop feedback matrix
u = body-axis forward velocity, ft/s
$\boldsymbol{u}$ = control vector
$\boldsymbol{u}_c$ = closed-loop control vector
$\boldsymbol{u}_f$ = feedforward control vector
v = body-axis lateral velocity, ft/s
v_x = local-level forward velocity, ft/s
v_y = local-level lateral velocity, ft/s
w = body-axis vertical velocity, ft/s
$\boldsymbol{x}$ = state vector
$\boldsymbol{x}_I$ = controller state vector
$\boldsymbol{x}_P$ = plant state vector
$\boldsymbol{y}$ = measurement vector
$\boldsymbol{y}_c$ = command vector
$\boldsymbol{y}_m$ = model output vector
δ_{a1} = lateral cylic control, deg of blade
δ_{b1} = longitudinal cyclic control, deg of blade
δ_{th} = collective control, deg of blade
δ_{tr} = tail rotor control, deg of blade
β = sideslip angle, deg
θ = pitch attitude, rad
ϕ = roll attitude, rad
ψ = heading, rad

Presented as Paper 91-2751 at the AIAA Guidance, Navigation, and Control Conference, New Orleans, LA, Aug. 12-14, 1991; received Aug. 23, 1991; revision received Feb. 9, 1992; accepted for publication Feb. 15, 1992.

*MDC Fellow, Advanced Engineering, Bldg. 530 B345, 5000 E. McDowell Road. Associate Fellow AIAA.
†Engineering Specialist, Avionics and Flight Controls, Bldg. 530 B345, 5000 E. McDowell Road. Senior Member AIAA.

Introduction

IN this paper we are concerned with the design issues for an actively controlled, helicopter fly-by-wire system. Although the term "highly augmented" is used to describe this type of system, we are not certain that there is a generally accepted meaning for that term. Tischler[1] discusses the design of highly augmented helicopter flight control systems, with emphasis on the higher bandwidths needed to meet certain handling-quality-related response requirements. Bandwidth is certainly a key factor in the design issues discussed in our paper, but we expand the scope of highly augmented to encompass flying quality features that go beyond those usually associated with meeting specification requirements, such as those found in ADS-33.[2] Specifically, we refer to the tight stabilization of all aircraft states associated with the six rigid-body degrees of freedom. That tight stabilization includes continuous automatic trimming to reduce errors in all commanded aircraft states to near zero. Thus, in our definition of highly augmented, piloting workload associated with stabilizing and trimming the aircraft is dramatically reduced. Pilot control inputs are used only to command changes to aircraft states. Release of the control input results in holding the existing states. Typically, these states may be attitude, heading, or velocity vector, depending on the control mode. In effect, a high-gain autopilot is continuously in the loop, without impeding aircraft maneuverability or agility. The aircraft can be flown to its performance boundaries without pilot concern over exceeding those boundaries. This capability taxes the system bandwidth issues noted by Tischler,[1] but low-frequency control associated with accuracy and automatic trimming must also be accomplished. Low-frequency control requires appropriate use of control law integrators and is an area that tends to be neglected in much of the literature on helicopter flight control design. In this paper, we review some of the multiple-input, multiple-output (MIMO) techniques needed to accomplish such a highly augmented system design, using the AH-64 Apache helicopter as the test bed.

Modern control methods for MIMO designs assume the plant and controller to be linear, finite-dimensional, time-invariant, and modeled by a rational transfer function matrix. A design synthesized using these assumptions should be validated for robustness against a more faithful representation of the plant and a more demanding, varying, and realistic set of operating conditions. In this paper, we do not explore the

validity of control theory applied to helicopter flight control, but rather show how practical robustness testing should be accomplished to validate a design. This practical testing not only attempts to verify that the system is stable for all expected variations in plant dynamics, but also that good performance is achieved as the nonlinear dynamic effects are encountered. This paper shows that systems can be stable but still provide unacceptable performance because of time-varying dynamics and other dominating nonlinear effects.

Tischler[1,3] addresses many of the practical issues associated with achieving high-gain, high-bandwidth control, emphasizing the source of system phase lags and the need for appropriate modeling of the higher-frequency part of the control loops. Hoffman et al.[4] relate cost functions of modern control methods to frequency domain performance criteria, using the CH-47 as the design example. The use of frequency domain representations with modern control to quantify bandwidth constraints became prevalent in the early 1980s[5] and techniques to improve design robustness continue to be researched.[6] Linearized equations around a trim point rapidly become invalid during aggressive maneuvers of the type required to show compliance with some handling-quality criteria defined in ADS-33.[2] So-called optimal solutions for controller gain matrices based on a linear model have no meaning during such typical maneuvers. Holdrige et al.[7,8] had the opportunity to flight test optimal flight control designs on the CH-47 and showed that systematic methods for adjusting elements in the weighting matrices were not available, and that the process used to match quadratic performance indices to the pilot's desired responses could be described as ad hoc.

A contention of this paper is that the design procedures for helicopter flight control, whether based on modern control methodologies or ad hoc methods, must recognize that the perturbation equations underlying the assumed plant dynamic models do not represent adequately the plant dynamics for a practical system design. Robustness of the design can only be achieved through high closed-loop gains, as noted in the work of Horowitz et al.[9-11] Although singular-value criteria and variations of such criteria that allow frequency weighting[5,6] can provide some insight into stability boundaries, they do not address performance issues related to a variety of phenomena, including the effect of the inherent nonlinearities. In this paper, we summarize the design procedures that produced a robust, full-envelope, fly-by-wire flight control system that has been fully validated in manned simulations and in flight on an AH-64 aircraft. Those procedures offer physical insight into the design process by featuring a decoupling technique that immediately converts the MIMO problem into a sequence of single-input, single-output (SISO) designs. The resulting performance meets the automatic trimming requirement noted previously. Other designs[12,13] for the same aircraft have appeared in the literature, and the performance of these other designs against practical test criteria is discussed. It is shown that these designs provide excellent results at the reference perturbation conditions, but fail robustness tests that require highly stable, automatic trimming in the presence of realistic nonlinearities.

Baseline Design: Model-Following Flight-Path Vector Control System

Figure 1 illustrates the type of explicit model-following concept used in the baseline design. It differs somewhat from the model-following configuration described by Tischler.[1] The basic difference is that no separate control loops are closed around the plant dynamics. The controller $G_c(s)$ contains the needed compensations and integrations consistent with the highest gains attainable within sensor measurement, actuator bandwidth, and rotor dynamic contraints. Because of effective time delays associated with sensor filtering and the inherent delays in the rotor's ability to generate the desired forces and moments needed to control the aircraft state vector, a sufficiently high gain in $G_c(s)$ is usually unattainable for assuring precise model-tracking. Hence, a feedforward is used that, ideally, assures zero error in the tracking loop. From Fig. 1, the response/command transfer function is

$$\frac{y}{y_c} = \frac{CHG_c + CHF}{1 + CHG_c} G_m \tag{1}$$

In the ideal, when $F = (CH)^{-1}$, this reduces to $y/y_c = G_m$, which says that the command response is completely determined by the model. One can compute the ideal feedforward control vector u_f that will produce the desired response, but we usually do not know H well enough to achieve the ideal plant inverse in this computation. However, as noted by Tischler,[1] an approximation of the plant inverse suffices to give good performance.

A key principle of the concept illustrated in Fig. 1 is the need for maximum attainable gains in G_c, despite the fact that a perfect response is attainable with $G_c = 0$ when we have an ideal feedforward solution. The rationale for high feedback gains is to make system response invariant with plant uncertainty and achieve a high level of disturbance attenuation. G_c determines the disturbance response characteristics and is designed for good gust rejection and high damping. If a disturbance D enters the plant through H in Fig. 1, then the disturbance transfer function is

$$\frac{x(s)}{D(s)} = \frac{H(s)}{1 + G_c(s)H(s)} \approx \frac{1}{G_c(s)} \quad \text{for} \quad G_c(s)H(s) \gg 1 \tag{2}$$

A functional block diagram of the baseline control system used for low-speed flight, illustrated in Fig. 2, shows that the pilot's side-stick inputs are used to control the aircraft's velocity vector directly. Specifically, a stick displacement commands a rate of change of the velocity component managed by the respective controller displacement. The four control axes are $\dot{u}$, body-forward acceleration; $\dot{v}$, body lateral acceleration; $\dot{w}$, body vertical acceleration; and r, body yaw rate. When stick force/displacement returns to zero, the existing velocity reference at the time of stick release is maintained. (Actually, the flight-path-angle reference is maintained.) As the aircraft speed increases, modes are automatically transitioned so that turn coordination is provided, with lateral maneuvering changing to a rate command, attitude hold mode. The system can also smoothly transition into a three-axis attitude rate command mode for aerobatic capability. As seen in Fig. 2, the

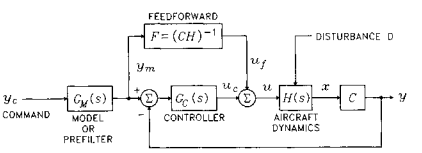

Fig. 1 Basic model-following concept.

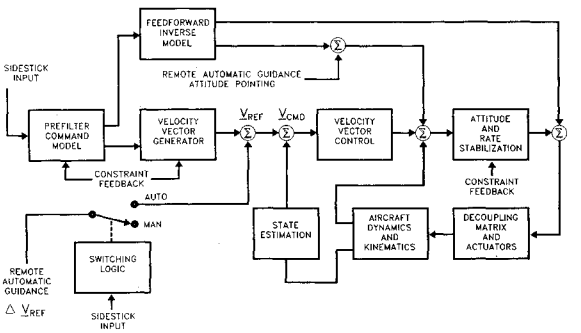

Fig. 2 Velocity vector fly-by-wire control with automated guidance capability.

attitude and attitude rate system is self-contained within the velocity vector system. The discussion of the flight modes and their flying qualities is covered in more detail by Morse.[14]

Figure 2 shows that velocity references can be generated from the pilot's stick inputs (as increments to the existing velocity reference) or from an automatic remote guidance function that can provide the equivalent of autopilot functions. Velocity errors are input to a velocity control law that contains proportional-plus integral terms and appropriate switching of the integral gains to prevent saturation-induced instabilities. To zero the velocity errors, the aircraft's attitude is modulated so that the velocity errors may be viewed as generating attitude commands. The constraint feedbacks shown in Fig. 2 are inputs derived from measurements and estimations of rotor rpm, engine torque, load factor, and impending blade stall, so that the aircraft can be flown to its performance boundaries in a "carefree" manner, thereby significantly reducing pilot workload.

The approach followed in synthesizing a robust implementation of Fig. 2 has been to maintain a clear physical representation of the system so that the designers never lose the insights needed to appreciate how the maximum gain (maximum bandwidth) control is being achieved. That insight requires that the MIMO problem be converted into a series of SISO, relatively decoupled problems. Although formal methodologies for such design techniques have been described,[11] the approach followed for the baseline system discussed here is based on the use of a force and moment decoupling matrix that separates the attitude/vertical velocity stabilization problem into four SISO loops. Figure 3 illustrates the attitude control structure obtained with this approach. The attitude command at the left of the figure is derived from the velocity loop control law. In the vertical axis, a vertical velocity reference command is analogous to the attitude command. G_2 contains the proportional-plus integral (plus lead-lag compensator if needed). Note that all loops in the longitudinal axis are sequentially closed so that the proportional gain of G_2 represents the inner control-loop bandwidth in rad/s. All feedforwards, which can be approximately estimated, are shown in the proper part of the control loop of Fig. 3 so that they retain physical significance.

The problem is essentially decoupled if we indeed have a control device that generates predominantly $\dot{q}_{\text{cmd}}$ commands for pitch, as well as $\dot{p}_{\text{cmd}}$, $\dot{w}_{\text{cmd}}$, and $\dot{r}_{\text{cmd}}$ for the roll, vertical, and yaw axes, respectively. The solution is to create a control strategy in which the control vector $\boldsymbol{u}$ becomes $\dot{\boldsymbol{x}}_{\text{cmd}}$. Since four control inputs allow four states to be independently controlled, the $\boldsymbol{B}$ matrix is partitioned to include only the four states selected for direct control, in this case, q, p, w, r. Control input decoupling is achieved by inverting the partitioned $\boldsymbol{B}$ matrix, $\boldsymbol{B_P}$, to obtain

$$\boldsymbol{u} = \boldsymbol{B_P}^{-1}\dot{\boldsymbol{x}}_{\text{cmd}} \tag{3}$$

$\boldsymbol{B}\boldsymbol{B_P}^{-1}$ is identity for the controlled states, but it also contains terms that drive $\dot{u}$ and $\dot{v}$ as a function of $\dot{\boldsymbol{x}}_{\text{cmd}}$. These terms are neglected in the inner loop, but are indirectly controlled through the inertial velocity outer-loop control laws as already described.

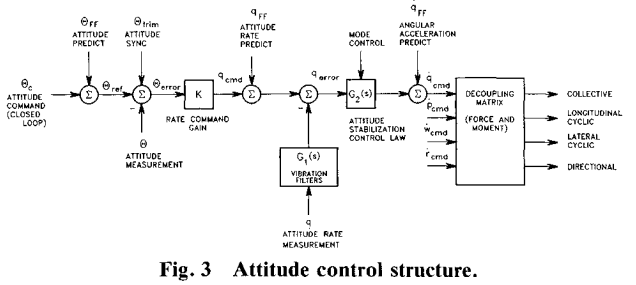

Fig. 3 Attitude control structure.

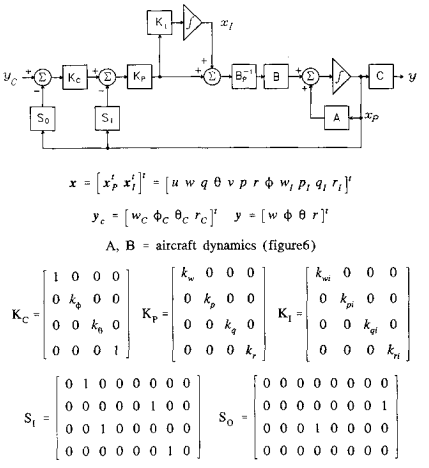

Fig. 4 Attitude and rate stabilization diagram.

Figure 4 summarizes the baseline flight control design, shown as a vector block diagram for the complete inner loop. The outer loops, which generate the velocity errors and heading errors, are not shown, but those loop errors are represented by the input vector y_c. The control feedback states w, p, q, r, ϕ, θ are available from contemporary strapdown inertial systems. The w state, however, generally requires some additional estimation functions.

Although Fig. 4 shows the basic inner-loop structure of the flight control system, the design problem for a practical system relates primarily to the management of mode synchronizations and initializations and constraints on the integrator gain matrix during large maneuvers and mode transitions. Stabilization gains defined by the $\boldsymbol{K_P}$, $\boldsymbol{K_I}$, and $\boldsymbol{K_C}$ gain matrices are nominally

$$\begin{aligned}
&\boldsymbol{K_P}: \quad k_w = 2 \quad k_p = 4 \quad k_q = 4 \quad k_r = 4 \\
&\boldsymbol{K_I}: \quad k_{wi} = 0.5 \quad k_{pi} = 3 \quad k_{qi} = 1 \quad k_{ri} = 0.5 \\
&\boldsymbol{K_C}: \quad k_\phi = 1 \quad k_\theta = 1
\end{aligned} \tag{4}$$

where $\boldsymbol{K_P}$ represents the inner-loop bandwidths and $\boldsymbol{K_I}$ contributes to steady-state accuracy and automatic trimming.

The design procedure is as follows:

1) Select a nominal bandwidth below that desired. A gain of 1.0 or 2.0 for each axis is a good start. (If we tried to close the control loop for one axis with the other loops open, we would encounter some difficult stability and often nonminimum phase problems that can be avoided by simultaneously closing all inner loops. The literature on MIMO techniques correctly notes this problem with SISO techniques.)

2) With this starting design, perform a SISO optimization on the pitch loop, attempting to increase the gain to the highest value consistent with practical sensor filter, actuator, and rotor dynamic delays. Maximum integral gains are set, and partial compensation for high-order dynamics may be used.

3) Increase the gain of the vertical SISO loop with the maximum gain of the pitch loop implemented.

4) Repeat this procedure for the roll and yaw loops.

5) With the maximum gain of all four SISO loops implemented, use Bode analysis to determine the resulting SISO gain and phase margins, seeking 6–10 dB gain margins and 30–45 deg phase margins.

6) With these inner loops optimized for maximum gain in this manner, close attitude and velocity loops as SISO problems. (They can indeed be considered SISO problems because of the strong decoupling that has already been achieved.) Again, choose the highest gains consistent with the gain and phase margin criteria. The gain settings for these loop closures do not determine the dynamic response to commands, since the model dynamics define that response characteristic. High gains are desired to achieve good disturbance responses.

7) The procedure just described starts with A and B matrix values for the hover condition. The decoupling matrix defined by inverting the B matrix must be scheduled for changing speed conditions. After adjusting the decoupling matrix for various forward and lateral speed conditions, the baseline gains are tested for the changing A and B matrices and appropriate gain schedules defined.

Validation of the Linear Perturbation Model

The baseline system design was developed for an experimental fly-by-wire system implemented on an AH-64 attack helicopter. Complete nonlinear simulation models, validated against the real aircraft, were available to support the testing of the design on a manned simulator. In addition, perturbation models at various flight conditions were determined from in-flight frequency sweeps. The flexural frequencies, identified by in-flight frequency sweeps, are significant for estimating gain margins in a wide-bandwidth control system, but are, in general, not needed for high-fidelity manned simulations.

Figure 5 illustrates the perturbation model for this aircraft, with the rigid-body linear perturbation equation for the hover flight condition shown in Fig. 6. Note that flexure dynamics were matched to p, q, and r attitude rate measurements at the location of the aircraft's inertial measurement unit. Rotor dynamics are approximations, with a Padé representation of the time delay that dominates. Actuator dynamics are linear approximations of the flight equipment, although saturation and load effects are not included in this simplified model. Anti-aliasing and notch filters used with the angular-rate sensor measurements, $G_I(s)$ in Fig. 3, contribute phase delays of the same order as the actuator dynamics and are included in the analytical models.

Testing Control Designs for Performance and Robustness

System designs require exhaustive testing to verify that unusual regions of instability or performance deterioration do not exist within the flight envelope. Manned simulations using complete nonlinear models of the aircraft are the primary means of achieving that verification. Since the manned simulations do not usually include the higher-order dynamics associated with such phenomena as elastic modes and sensor vibration/anti-aliasing filters, a parallel effort is needed to determine a more accurate measure of the high-frequency bandwidth-limiting criteria such as system phase and gain margins. This latter analysis is done with the linearized models, but it must include realistic provisions for significant variations that will occur in the A and B matrix elements. Thus, the first step in robustness testing is to define phase and gain margins with matrix element variations that can exceed 100%. Magnitudes of these variations are determined from known physical sensitivities, such as variations with thrust, sideslip, impending rotor blade stall, and rotor droop. Combinations are inserted into the model at random, and simple transient response or phase/gain margin deteriorations are explored. These preliminary tests allow refinement of designs to address unique problem areas that might exist under realistic conditions.

Following these refinements using the high-order, linear perturbation model, the design is exposed to the full nonlinear aircraft model and required to perform severe maneuvers, including those at the aircraft's performance boundaries. One of these maneuvers is a sequence of elliptical turns during which sideslip varies through ±180 deg. Performance of the baseline design described in this paper, when subjected to this elliptical turn test, will be discussed subsequently.

It would be informative to explore the differences between the procedures just described and the results given by formal robustness criteria. Two published papers have used the identical model defined in Figs. 5 and 6, so that the results provided by designs presented in those papers can be used to illustrate some of the performance issues that we have been noting. Garrard et al.[12] used the AH-64 model to illustrate an attitude control design based on eigenstructure assignment, and Ekblad[13] describes a velocity control extension of this technique. Both designs met singular-value criteria for robustness. They will not, however, meet the performance requirements that we have established for a highly augmented system. Their objectives were to alter the behavior of the basic helicopter so that specified attitude or velocity responses are obtained. Their methodology uses full state feedback to cancel the basic aircraft poles (with zeros) and places poles in the s plane such that the desired dynamic response is obtained. However, neither of these two designs addresses the tight stabilization or automatic low-frequency trimming that we have noted as requirements for a highly augmented system. The difference between these

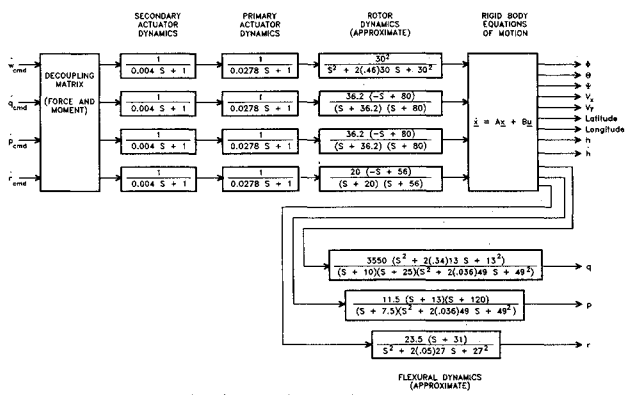

Fig. 5 System interconnection: actuators, rotor, and flexural dynamics.

$$\begin{bmatrix} \dot{u} \\ \dot{w} \\ \dot{q} \\ \dot{\theta} \\ \dot{v} \\ \dot{p} \\ \dot{r} \\ \dot{\phi} \end{bmatrix} = \begin{bmatrix} -.0286 & .0205 & 7.97 & -32.0 & -.0637 & .229 & -.257 & 0 \\ .00463 & -.261 & 2.25 & -3.28 & -.0257 & -.379 & 2.19 & 1.60 \\ .00473 & .00016 & -0.75 & 0 & .0118 & -.00915 & .0244 & 0 \\ 0 & 0 & .999 & 0 & 0 & 0 & .0499 & 0 \\ .0779 & .00593 & -1.03 & .164 & -.231 & -8.29 & -1.64 & 32.0 \\ .00793 & .00952 & -.134 & 0 & -.05 & -2.7 & -.662 & 0 \\ .00393 & .0008 & .413 & 0 & -.0049 & -1.05 & -.4 & 0 \\ 0 & 0 & -.00513 & 0 & 0 & 1.0 & .103 & 0 \end{bmatrix} \begin{bmatrix} u \\ w \\ q \\ \theta \\ v \\ p \\ r \\ \phi \end{bmatrix} + \begin{bmatrix} .435 & .576 & -.114 & -.00086 \\ -4.27 & .0575 & -.025 & .00118 \\ .0072 & -.101 & -.09 & -.00187 \\ 0 & 0 & 0 & 0 \\ -.158 & .136 & .491 & .282 \\ -.0438 & -.06 & .647 & .08 \\ .08 & .00973 & .2 & -.0455 \\ 0 & 0 & 0 & 0 \end{bmatrix} \begin{bmatrix} \delta_{ch} \\ \delta_{h1} \\ \delta_{a1} \\ \delta_{tr} \end{bmatrix}$$

Fig. 6 Hover linear perturbation model.

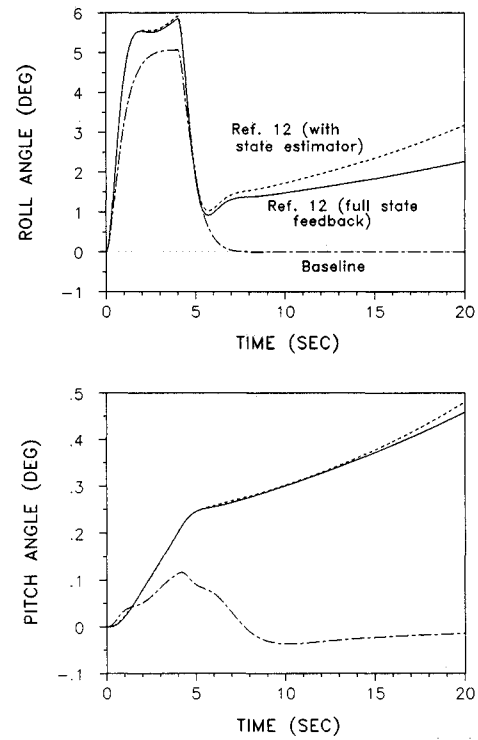

Fig. 7 Reference 12 performance vs baseline design with 20% increase in B_{63}.

variable stability designs and a tightly stabilized system will now be described.

With the nominal values of the A and B matrices for the hover flight condition, Garrard's[12] design provides excellent roll command response, achieving the specified attitude response criteria. However, if we change the rolling moment effectiveness coefficient in the B matrix by +20%, we observe in Fig. 7 that the roll attitude begins to drift from its commanded value. Figure 7 shows a 4-s step command response for this very benign alteration in a plant parameter, comparing the Ref. 12 design with the baseline highly augmented system described in this paper. The highly augmented design showed no change in response, precisely achieving the 5-deg command and returning to zero when the command was released. The Ref. 12 design continues to meet its attitude command response flying-quality objective, but requires pilot participation in maintaining aircraft trim. The need for aircraft trim results from a closed-loop right-half-plane pole that appears in the ϕ/δ_{al} transfer function because of the change in the B matrix parameter.

Of greater significance than this trimming issue is the concept of tight stabilization. This can be demonstrated by inserting a disturbance moment of relatively benign magnitude (equivalent to 5 deg/s^2). Figure 8 compares the baseline highly augmented system response with the Ref. 12 response, using the original A and B matrices in the aircraft model. Note that the baseline design suppresses this disturbance moment, developing an appropriate lateral cyclic command to maintain zero roll attitude. The Ref. 12 design develops a small lateral cyclic

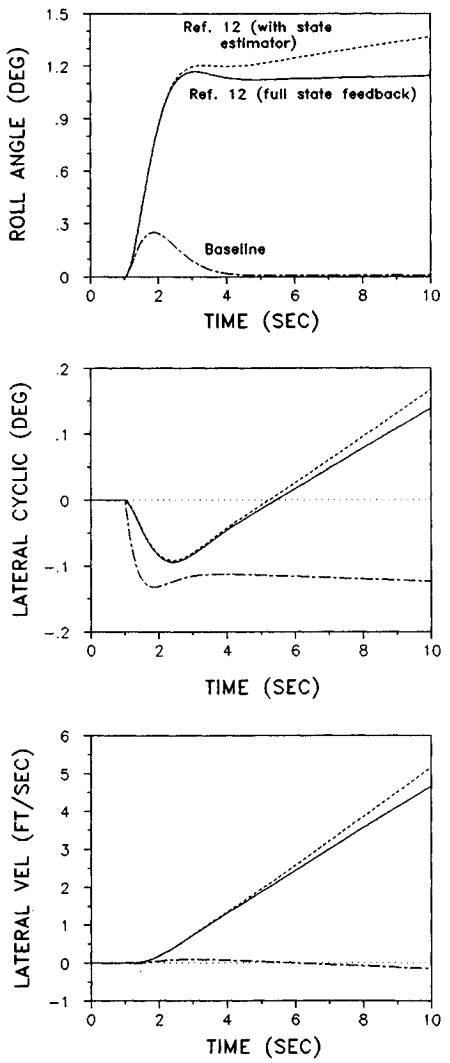

Fig. 8 Reference 12 vs baseline disturbance rejection performance.

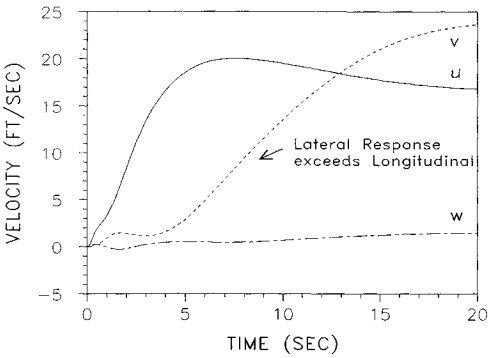

Fig. 9 Reference 13 20-ft/s response with nonlinear model.

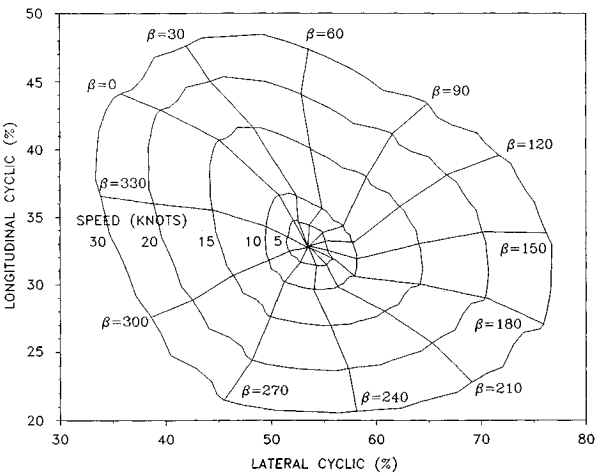

Fig. 10 Control trim map as a function of speed and sideslip angle.

that starts to oppose the disturbance, but then reverses direction in responding to a lateral velocity drift. There is a resulting roll attitude error plus lateral velocity drift. Note that the baseline design shows an imperceptible lateral velocity error, but even that error would be suppressed if we closed the velocity outer loop of the system. If we included the 20% change in the B matrix, the baseline response is essentially unchanged, although it shows a lower magnitude roll error because the roll gain is increased by this specific B matrix change. The Ref. 12 response will add the slow roll divergence to the offsets and drifts illustrated in Fig. 8. Even with these drifts and offsets, the Ref. 12 results described in Fig. 7 do not preclude that design from meeting ADS-33[2] handling-quality specifications. This point illustrates that even recent handling-quality specifications such as ADS-33 do not recognize the very significant work load reduction potential in the type of system that we have referred to as highly augmented.

The Ref. 13 design was tested against the nonlinear model. First, a 2-ft/s forward velocity step command was inserted from a hover trim condition. Results were essentially identical to those obtained with the perturbation model, since a 2-ft/s change in velocity is readily accommodated by the linearized model. The command was then increased to 20 ft/s. With the linear plant model, all responses are scaled upward by a factor of 10. With the nonlinear plant model, a long-term anomaly appeared. Figure 9 illustrates the response. While the longitudinal velocity u response starts out in accordance with the design objective, a long-term lateral velocity v develops, exceeding the commanded longitudinal velocity after about 12 s. This problem is not caused by control saturation or excessive attitude maneuvers.

The problem is apparently caused by a large directional control error with a significant steady-state yaw rate. Again, this problem results from a system that is not sufficiently stabilized to maintain and trim all the states to their commanded values.

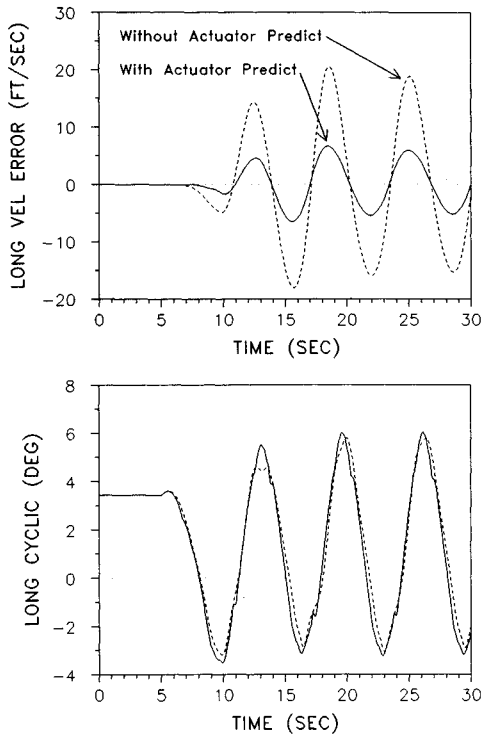

Fig. 11 Baseline design subject to elliptical turn test.

Finally, let us consider test procedures to measure system performance when severe trim changes would normally occur. The baseline design uses high-gain integrations and feedforward compensators to correct for such large excursions from trim conditions. It will be shown that these techniques should be augmented with trim tables that feed into the feedforward loops of Fig. 3.

In the baseline design, the reference velocity vector is maintained in inertial space. Thus, if a north velocity reference of 30 kts and an east and vertical velocity reference of zero are established, the aircraft will be controlled to maintain the reference velocity vector, regardless of where the nose is pointed. The robustness test, therefore, establishes a north velocity reference of 30 kts while the aircraft is pointed north. Next, a body yaw rate of 1.0 rad/s is inserted to rotate the aircraft about its Z axis while trying to maintain the inertial velocity vector reference. This requires that the aircraft be flown through ± 180 deg of sideslip. Aerodynamic effects of sideslip excursions are significant, and the linearized perturbation equations are certainly not a valid representation of the control problem under these conditions. Figure 10 shows a trim map for lateral and longitudinal cyclic controls through such sideslip changes. Note that a significant part of the full control authority is needed to maintain the aircraft in any instantaneous sideslip condition. When sideslip varies through ± 180 deg in a 6.28-s period, the control activity is significant.

Figure 11 shows baseline system performance during this type of maneuver. Results with and without the trim predictor tables are shown. Without the trim compensation, we are dependent on the closed-loop velocity error feedback plus the feedforward that predicts the changing pitch and roll attitude as a function of forward and side velocity, but the closed-loop bandwidth for tracking the rapidly changing velocity references are not adequate for good performance. Even with the trim feedforward compensations derived from Fig. 10, significant instantaneous body-referenced velocity errors are seen in Fig. 11. This figure demonstrates that the design is robust from a practical viewpoint, but not necessarily optimum in regard to error minimization. Robustness testing performed in the manner described in this paper provided confidence that the flight system would not experience unforeseen performance or stability problems.

Conclusions

A highly augmented flight control system has been defined as one that maintains tight stabilization of all commanded states, including automatic trimming of low-frequency dynamic effects. A practical process for designing such multiple-input, multiple-output helicopter systems starts by decoupling controls into four single-input single-output axes, with the control bandwidth represented as a clear, physically significant gain matrix. Linear perturbation models used in helicopter flight control system designs are not sufficient to establish the practical robustness of those designs, especially in the area of low-frequency instabilities. Highly augmented flight control systems require high-gain/high-bandwidth control loops augmented by appropriate feedforward compensators, partially based on approximating the aircraft plant inverse model. Practical robustness tests needed to validate such designs should use the full nonlinear plant model, with maneuver tests that exercise the system throughout the maneuvering flight envelope, such as through ± 180 deg of sideslip in low-speed maneuvers, where regions of reduced stability or performance degradation may exist.

References

[1]Tischler, M. B., "Digital Control of Highly Augmented Combat Rotorcraft," NASA TM 88346 (USAAVSCOM Tech. Rept. 87-A-5), May 1987.

[2]U.S. Army Aviation Systems Command, *Aeronautical Design Standard, Handling Qualities Requirements for Military Rotorcraft*, ADS-33C, Aug. 1989.

[3]Tischler, M. B., "Assessment of Digital Flight Control Technology for Advanced Combat Rotorcraft," *Journal of the American Helicopter Society*, Vol. 34, No. 4, Oct. 1989.

[4]Hoffmann, L. G., Riedel, S. A., and McRuer, D., "Practical Optimal Flight Control System Design for Helicopter Aircraft," NASA CR 3275, Contract NAS2-9946, May 1980.

[5]Doyle, J. C., and Stein, G., "Multivariable Feedback Design: Concepts for a Classical/Modern Synthesis," *IEEE Transactions on Automatic Control*, Vol. AC-26, Feb. 1981.

[6]Stein, G., and Doyle, J. C., "Beyond Singular Values and Loop Shapes," *Journal of Guidance, Control, and Dynamics*, Vol. 14, No. 1, 1991, pp. 5-16.

[7]Holdridge, R. D., Hindson, W. S., and Bryson, A. E., "LQG—Design and Flight-Test of a Velocity-Command System for a Helicopter," AIAA Paper 85-1887, 1985.

[8]Holdridge, R. D., "A Modern Control Design Methodology with Application to the CH-47 Helicopter," Ph.D. Dissertation, Stanford Univ., SUDAAR 546, Stanford, CA, Jan. 1985.

[9]Horowitz, I. M., "Superiority of Transfer Function over State-Variable Methods in Linear Time Invariant Feedback System Design," *IEEE Transactions on Automatic Control*, Vol. AC-20, No. 1, 1975.

[10]Horowitz, I., Golubev, B., Kopelman, T., and Britman, S., "Research in Advanced Flight Control Design," AFFDL-TR-79-3120, Jan. 1980.

[11]Horowitz, I., and Kopelman, T., "Multivariable Flight Control Design with Uncertain Parameters," Tech. Rept. AFWAL-TR-83-3036, Wright-Patterson AFB, OH, Sept. 1982.

[12]Garrard, W. L., Low, E., and Proudy, S., "Design of Attitude and Rate Command Systems for Helicopters Using Eigenstructure Assignment," *Journal of Guidance, Control, and Dynamics*, Vol. 12, No. 6, 1989, pp. 783-791.

[13]Ekblad, M., "Reduced Order Modeling and Controller Design for a High-Performance Helicopter," *Journal of Guidance, Control, and Dynamics*, Vol. 13, No. 3, 1990, pp. 439-449.

[14]Morse, C., "ADFCS and NOTAR, Two Ways to Flying Quality," AGARD Flight Mechanics Panel Symposium on Flying Qualities (Quebec), Oct. 15-18, 1990.